

# Fabrication of carbon fiber reinforced ceramic matrix composites with improved oxidation resistance using boron as active filler

Zhen Wang<sup>a</sup>, Shaoming Dong<sup>a,c,\*</sup>, Ping He<sup>a</sup>, Le Gao<sup>a</sup>, Haijun Zhou<sup>a,b</sup>,  
Jinshan Yang<sup>a,b</sup>, Dongliang Jiang<sup>a</sup>

<sup>a</sup> Structural Ceramics and Composites Engineering Research Center, Shanghai Institute of Ceramics,  
Chinese Academy of Sciences, 1295 Dingxi Rd, Shanghai 200050, PR China

<sup>b</sup> Graduate University of Chinese Academy of Sciences, Beijing 100049, PR China

<sup>c</sup> State Key Laboratory of High Performance Ceramics and Superfine Microstructure, Shanghai Institute of Ceramics,  
Chinese Academy of Sciences, 1295 Dingxi Rd, Shanghai 200050, PR China

Received 14 May 2009; received in revised form 8 September 2009; accepted 10 September 2009

Available online 4 October 2009

## Abstract

Boron was introduced into C<sub>f</sub>/SiC composites as active filler to shorten the processing time of PIP process and improve the oxidation resistance of composites. When heat-treated at 1800 °C in N<sub>2</sub> for 1 h, the density of composites with boron (C<sub>f</sub>/SiC-BN) increased from 1.71 to 1.78 g/cm<sup>3</sup>, while that of composites without boron (C<sub>f</sub>/SiC) decreased from 1.92 to 1.77 g/cm<sup>3</sup>. So when boron was used, two cycles of polymer impregnation and pyrolysis (PIP) could be reduced. Meanwhile, the oxidation resistance of composites was greatly improved with the incorporation of boron-bearing species. Most carbon fiber reinforcements in C<sub>f</sub>/SiC composite were burnt off when they were oxidized at 800 °C for 10 h. By contrast, only a small amount of carbon fibers in C<sub>f</sub>/SiC-BN composite were burnt off. Weight losses for C<sub>f</sub>/SiC composite and C<sub>f</sub>/SiC-BN composite were about 36 and 16 wt%, respectively.

© 2009 Elsevier Ltd. All rights reserved.

**Keywords:** Active filler; In situ reaction; Ceramic matrix composite; Oxidation resistance; Microstructure

## 1. Introduction

The most commonly used ceramic matrix composites (CMCs) are those comprising carbon or SiC fibers in a carbon or SiC matrix (C/C, C/SiC, SiC/SiC composites). C/SiC composites are potential candidates for a variety of applications in aerospace fields, including rocket nozzles, heat shields and aeronautic jet engines.<sup>1,2</sup> However, the principal obstacle for wider applications, especially for long-term applications, of carbon-containing materials is known to be their relatively poor oxidation resistance.<sup>3</sup> Oxidation of carbon starts at temperatures as low as 450 °C, and its lifetime is dramatically limited beyond this temperature. The lifetime of CMCs which are partly made of carbon is strongly depended on the efficiency of the anti-oxidation systems used to reduce the oxygen permeability.<sup>4</sup> Extensive studies have been undertaken to improve the oxidation

resistance of carbon fiber reinforced CMCs and most are related to the application of boron-bearing species.<sup>5–8</sup> One important property of boron-bearing species is to form fluid oxide phases (B<sub>2</sub>O<sub>3</sub> or B–M–O ternary phase) over a broad temperature range (600–1200 °C for B<sub>2</sub>O<sub>3</sub>) when heated in an oxidizing atmosphere.<sup>9</sup> Compared to multilayered self-sealing matrix fabricated by CVI method,<sup>7</sup> boron-based particles introduced by slurry infiltration method have shortened the processing time and lowered the processing cost. A simple way to introduce boron-based particles is to impregnate a fiber perform with slurry consisting of boron-based particles.<sup>10</sup>

In the present work, carbon fiber reinforced ceramic matrix composites were fabricated by active-filler-controlled polymer pyrolysis (AFCOP) process.<sup>11</sup> Boron was introduced into the carbon fiber bundles as active filler to form some boron-bearing species by in situ reactions during the heat-treatment process. The influences of boron on microstructures as well as the oxidation resistance of the composites were studied in comparison with those of C<sub>f</sub>/SiC composites fabricated by PIP using SiC particles as inert filler.

\* Corresponding author. Tel.: +86 21 52414324; fax: +86 21 52413903.  
E-mail address: [smdong@mail.sic.ac.cn](mailto:smdong@mail.sic.ac.cn) (S. Dong).

Table 1  
Properties of the carbon fiber reinforced ceramic matrix composites.

Sample	Raw material ratio (wt%)	Fiber fraction (%)	Density ( $\text{g cm}^{-3}$ )	Open porosity (%)	Bending stress (MPa)	Elastic modulus (GPa)
S	55(SiC)+45(PCS)	45%	2.11	7.2	$88.5 \pm 30.4$	$60.9 \pm 4.5$
S*	45(B)+55(PCS)	44%	1.98	8.4	$86.5 \pm 9.6$	$52.5 \pm 4.5$

## 2. Experimental procedure

Nano-SiC (Kai'er Nanometer Technology Development Co., Ltd., Hefei, China) or boron (Tangshan WeiHao Magnesium Powder Co., Ltd., Tangshan, China) powders were mixed with PCS (National University of Defense Technology, Changsha, China) by ball-milling for 48 h, using xylene as solvent to form homogenous slurries. Table 1 listed the ratios of raw materials in the slurries. 2D woven carbon fiber plain fabrics (Mitsubishi Rayon,  $200 \text{ g/m}^2$ ) were first deposited with PyC interphase at  $1050^\circ\text{C}$  using methane as precursor and the average thickness of the PyC interphase is about 100 nm. The source gases were first introduced into the reaction chamber with a pressure of 10 kPa, then the exhausts were evacuated to below 300 Pa using vacuum pumps within 5 s after holding for 20 s at  $1050^\circ\text{C}$ . The coated fabrics were impregnated with the aforementioned slurries and stacked in a graphite die after drying. Pressures were applied to control their thicknesses according to a fiber volume of about 45% in the hot-pressing furnace at  $200^\circ\text{C}$ . Composite derived from the boron-containing slurry was denoted as S\* and the other was denoted as S. After further densified by several cycles of PIP (5 cycles for S and 3 cycles for S\*) using PCS as the polymer with the pyrolysis temperature of  $800^\circ\text{C}$ , the samples were heat-treated (nitrided) at  $1800^\circ\text{C}$  in  $\text{N}_2$  atmosphere for 1 h. Then PIP was performed again to fill the open pores with the pyrolysis temperature of  $1100^\circ\text{C}$ .

After being cut and ground into  $5 \text{ mm} \times 2 \text{ mm} \times 20 \text{ mm}$ , the specimens were deposited with a SiC coating of about  $10 \mu\text{m}$  by CVD to isolate the cross-sections from the air for oxidation. SiC coating was deposited at  $1100^\circ\text{C}$  and 5 kPa using MTS and  $\text{H}_2$  as source gases with the molar ration of  $\text{H}_2$  to MTS was 10. Oxidation tests were performed in a muffle furnace. The specimens were pushed into the furnace when the temperature reached  $800^\circ\text{C}$  and then taken out quickly to weight the mass after each 2.5 h oxidation. The weight losses of composites in air from room temperature to  $1000^\circ\text{C}$  were also measured by TG.

The densities and open porosities of samples were measured by the Archimedes method. Mechanical properties were measured by three-point-bending tests with  $5 \text{ mm} \times 2 \text{ mm} \times 40 \text{ mm}$  specimens in an Instron-5566 machine, operated at a crosshead speed of 0.5 mm/min and a span of 24 mm. The microstructures of composites both before and after oxidation were observed by electron probe microanalyzer (EPMA, JXA-8100, JEOL, Tokyo, Japan) equipped with wave-length dispersive spectroscopy (WDS).

## 3. Results and discussion

The properties of both composites are summarized in Table 1. It can be obtained that the density of composite S is higher

than that of S\*. This may be a result of lower density of h-BN ( $2.27 \text{ g/cm}^3$ ) than that of SiC ( $3.20 \text{ g/cm}^3$ ). It is also indicated that composite S\* has a lower elastic modulus though there is only very small difference in the bending stresses, which may be accounted by the introduced h-BN into composites and h-BN is often introduced into composites to decrease their elastic modulus.<sup>12–14</sup>

The densities of samples after each PIP cycle are calculated according to their weights and volume in that there is almost no change in the volumes of samples in both PIP process and nitridation process. The density variation versus PIP cycles is plotted in Fig. 1. It is interesting to find from these two curves that the introduction of active fillers has a strong influence on the densification process of the composites. In the nitridation process, the density of S decreases from 1.92 to  $1.77 \text{ g/cm}^3$  while that of S\* increases from 1.71 to  $1.78 \text{ g/cm}^3$ . The density decrease of S may be caused by the weight loss of carbon fibers and decomposition of Si–O–C existing in the matrix. The fiber reinforcements used in this work will lose some active components when the fibers were heat-treated at high temperature and the weight loss is about 3.5%. In addition, as a result of the oxygen introduced into the PCS structure during its synthesis, Si–O–C phase will be formed. At temperatures higher than  $1400^\circ\text{C}$ , decomposition of amorphous Si–O–C phase begins with the evolution of CO and SiO.<sup>15</sup> When S\* is concerned, boron will react with

Table 2  
Changes in density and open porosity for both composite S and S\* occurring in the nitridation process.

Sample	Density ( $\text{g cm}^{-3}$ )		Open porosity (%)	
	Before	After	Before	After
S	1.92	1.77	8.7	24.7
S*	1.71	1.78	12.2	20

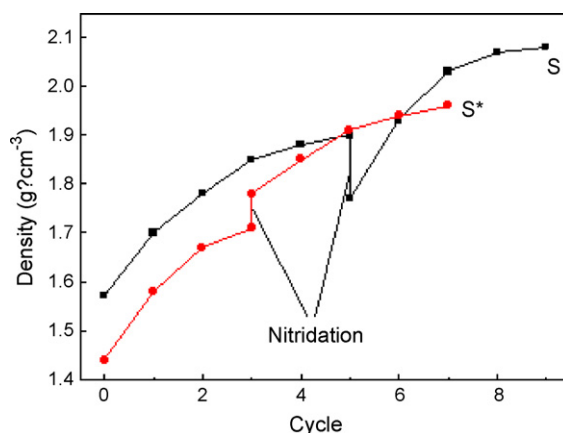


Fig. 1. Influences of boron on the density variations of composites.

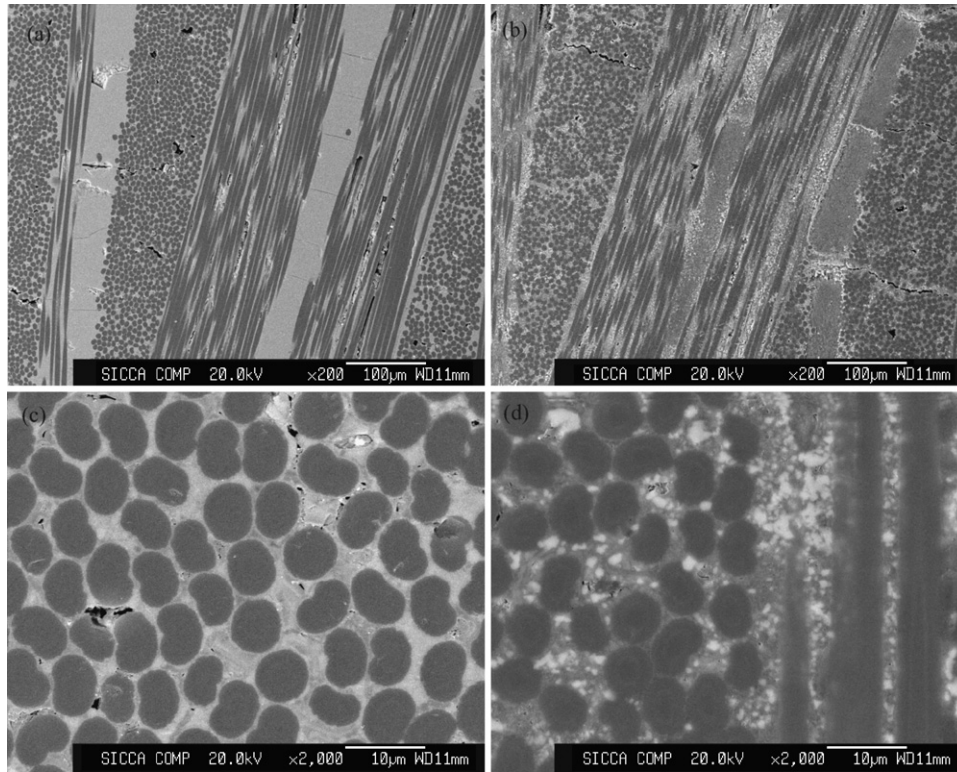


Fig. 2. Back-scattered electron images on the polished cross-sections of the composites (a, c: S; b, d: S\*).

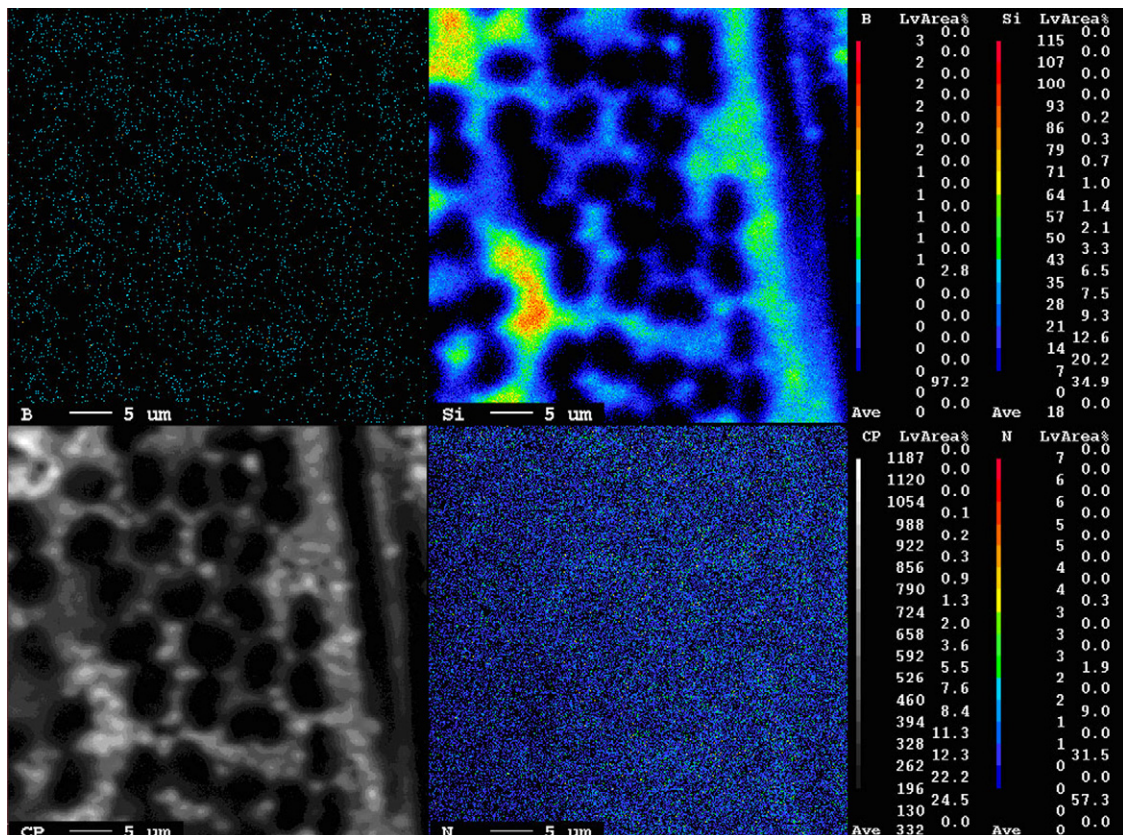


Fig. 3. WDS analysis of composite S\*.



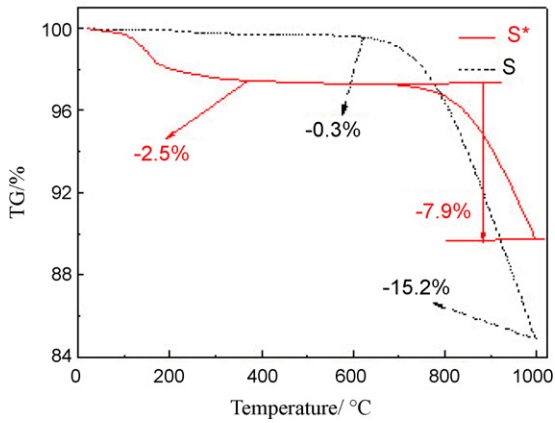


Fig. 4. Bending stress–displacement curves for composites.

the decomposition product and/or protective gas and the weight gain occurring in reaction will offset the weight loss induced by the decomposition of carbon fibers and Si–O–C. There is a mass gain of about 130% in the nitridation of boron according to the reaction between boron and nitrogen. On the other hand, as reported by Greil<sup>11</sup> the volume expansions in boron carbonization and nitridation process are 20 and 142%, respectively, which can compensate the volume shrinkage during PCS pyrolysis and crystallization process and account for the reduced PIP cycles. As it can be found from Table 2 that the open porosity of composite S increased by 16% while that for composite S\* just increased by 7.8%. The increase of open porosity may result from the decomposition of Si–O–C and conversion of close pores into open pores and the less increase of open poros-

ity for C<sub>f</sub>/SiC–BN composites may be an evidence of the filling of pores by the formed h-BN.

As can be observed from the micrographs of polished cross-sections shown in Fig. 2, most areas are dense but some residual pores and cracks remain in the intra-bundle areas in both composites. This can be attributed to the volume shrinkage accompanied in both ceramic conversion process and crystallization process, which will induce a large number of pores. It is also shown in the back-scattered electron images that the matrix of composite S\* has two phases with different contrast, which means there are some light elements in the dark one. According to the WDS analysis map of composite S\* (Fig. 3), the bright phase is mainly SiC while the dark is a mixture of SiC and h-BN. Meanwhile, it can be found from the dispersion maps of boron and nitrogen that the distribution of h-BN is homogenous in the matrix except in the bright phases, which correspond to SiC resulted from the followed PIP densification process. According to the chemical analysis results, the volume fraction of h-BN is about 22%.

It is indicated by the bending stress–displacement curves shown in Fig. 4 that both composites show a non-brittle fracture behavior. However, the bending stresses for both composites are relatively low. This may be ascribed to the degradation of fiber reinforcements. The escape of active groups leaves some small pores in the fibers and destroys the fibers' structure. Consequently, the strength of fiber reinforcements will drop dramatically, which is disadvantageous to the strength and toughness of composites. Only few and short pulled-out fibers can be observed on the fracture surface of both C<sub>f</sub>/SiC composite and C<sub>f</sub>/SiC–BN composite, as shown in Fig. 5. However, some layered crystal

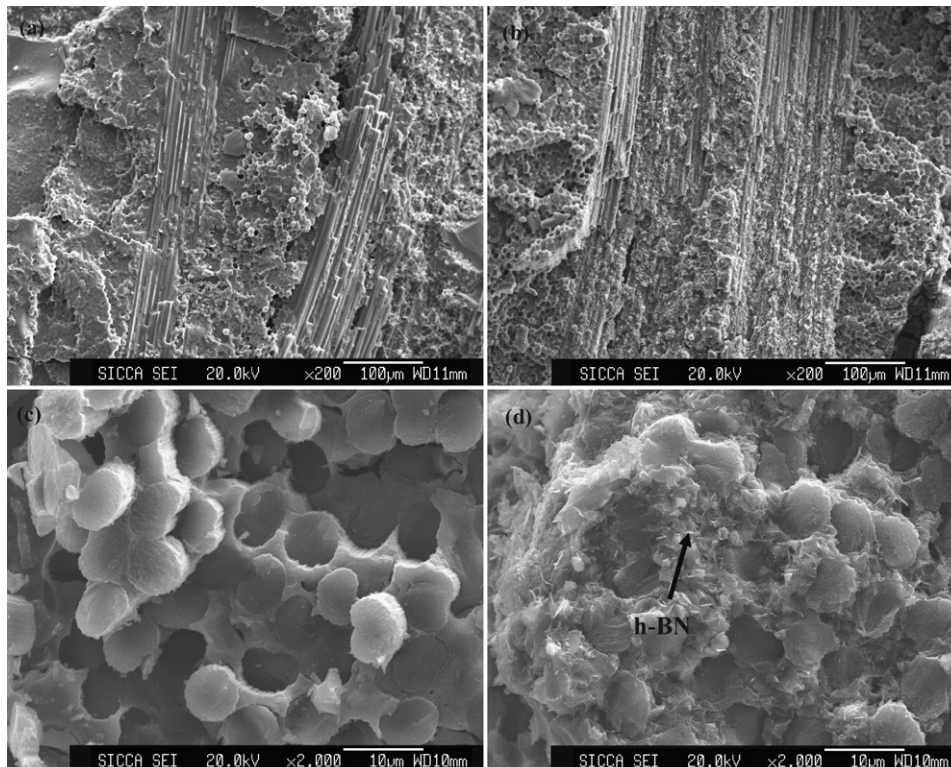


Fig. 5. SEM micrographs on the fracture surfaces of composites (a, c: S; b, d: S\*).

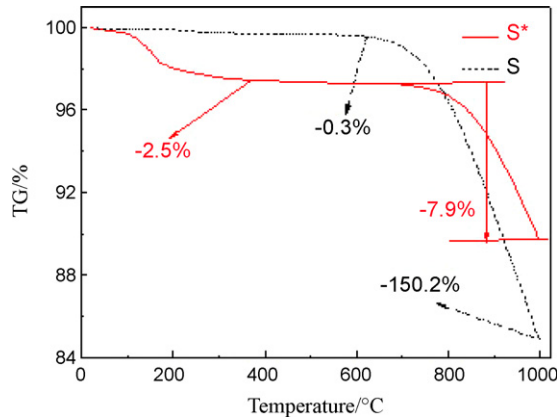


Fig. 6. TG curves of 2D  $C_f/SiC(-BN)$  composites in air from room temperature to 1000 °C.

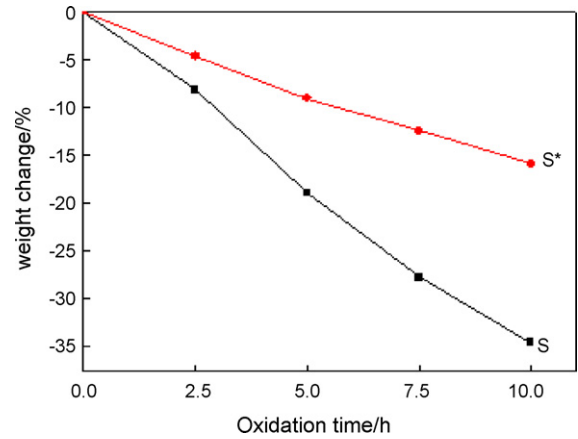


Fig. 7. Influences of boron on the weight changes of composites oxidized at 800 °C.

structure of flaked h-BN can be found in the matrix of composite  $S^*$ , as marked with the arrow. This phenomenon may be originated from the effect of h-BN on the crack propagation. h-BN has a layered structure similar to graphite, with a strong bonding within each layer and a weak bonding between the layers. When the crack tip contacts the h-BN particle, cracks will propagate along the interlayer within the h-BN grains.<sup>16,17</sup> Meanwhile, it can also be observed from the distribution of element silicon shown in Fig. 3 that there is a low concentration of silicon in the outer region of carbon fibers, which indicates the diffusion of silicon into carbon fibers. The diffusion of silicon into fibers may lead to destroy of their structures, which also accounts for the short length of pulled-out fibers.

Fig. 6 shows the TG curves of both  $C_f/SiC$  composite and  $C_f/SiC-BN$  composite in air from room temperatures to 1000 °C with the heating rate of 5 °C/min. It can be found by comparing the TG curve of  $C_f/SiC-BN$  composites with that of  $C_f/SiC$  composite, weight loss takes place at temperature below 300 °C and the weight loss is about 2.5% while that for  $C_f/SiC$  composite is about 0.3%. In the nitridation process,  $N_2$  will first react with boron resulting in the formation of h-BN on the surface. As a consequence, the formed h-BN will block the diffusion of  $N_2$  and slow down the reaction rate. Therefore, when the boron particle is large, some boron will be left in the core of boron particles after nitridation. In the machining process, boron may react with water to form some boric acid ( $H_3BO_3$ ) when it

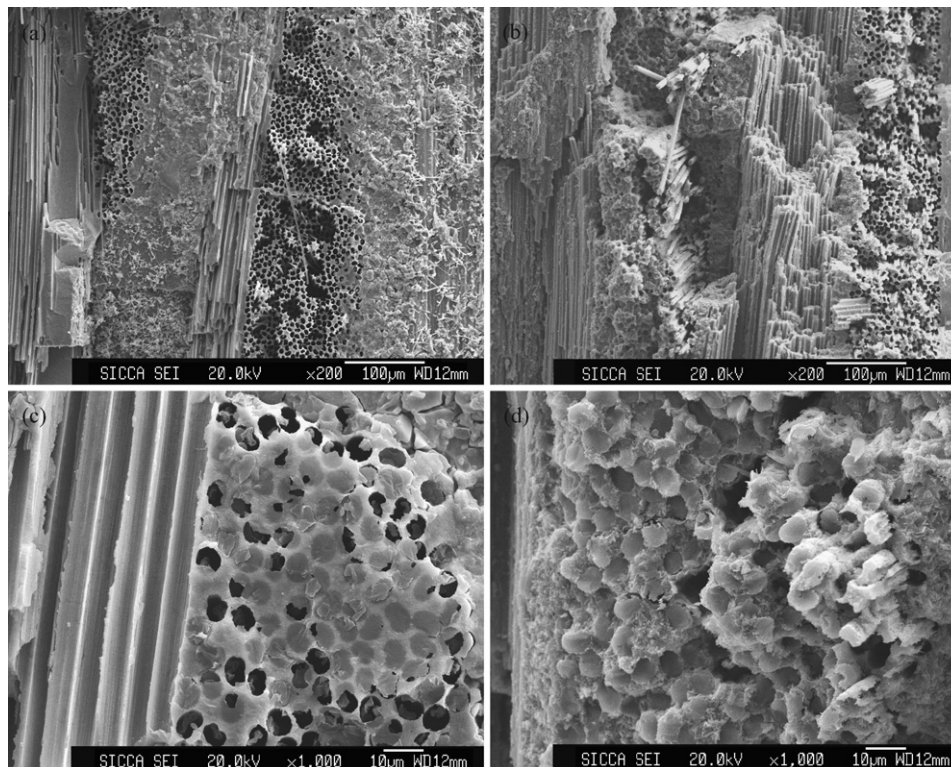


Fig. 8. Morphologies on the fracture surface of the composites after being oxidized at 800 °C for 10 h (a, c: S; b, d:  $S^*$ ).



contacts with water. When it is heated,  $H_3BO_3$  will decompose into  $B_2O_3$ , therefore, the weight loss of  $C_f/SiC$ -BN composites below  $300^\circ C$  may be mainly induced by the decomposition of  $H_3BO_3$ . At temperature above  $600^\circ C$ , carbon fibers and PyC interphases in  $C_f/SiC$  composite start to be oxidized, and the weight loss from 600 to  $1000^\circ C$  was about 14.9%. However, the weight loss of  $C_f/SiC$ -BN composite takes place at about  $700^\circ C$  and the weight loss from 700 to  $1000^\circ C$  is about 7.9%. When  $C_f/SiC$ -BN composites were heated at high temperature in air, both carbon phase and h-BN in the matrix will react with oxygen, which will cause weight loss and weight gain, respectively. Furthermore, the formed  $B_2O_3$  due to the oxidation of h-BN will slow down the diffusion rate of oxygen and lead to a lower oxidation rate and the weight gain accompanied in the h-BN oxidation process will compensate the weight loss caused by oxidation of carbon fibers.

Fig. 7 shows oxidation behavior of both composite S and  $S^*$  with a SiC layer of about  $10\ \mu m$  at  $800^\circ C$ . It can be concluded from these two curves that the longer the oxidation time is, the more weight both composites will lose. However, with the incorporation of boron-bearing species, the oxidation resistance of composite is greatly increased. When  $C_f/SiC$ -BN composite is oxidized at  $800^\circ C$ , h-BN will be oxidized and result in the formation of  $B_2O_3$ . As a result of its low melting temperature ( $450^\circ C$ ) and the volume expansion in the conversion from h-BN into  $B_2O_3$ ,  $B_2O_3$  fluid will fill into the micro-cracks and pores in the composites and decrease the in-depth diffusion of oxidative gases to the carbon phases (PyC interphase and carbon fibers).<sup>3,4,8</sup> When oxidized at  $800^\circ C$  for 10 h, most of the carbon fibers in composite S have been burnt off (Fig. 8a and c). Nevertheless, only a small amount of holes can be found in the fracture surface micrograph of oxidized  $S^*$ , most of the fibers remain intact or just partially oxidized (Fig. 8b and d). This is consistent with the less weight loss of  $C_f/SiC$ -BN composite (about 16 wt%) compared to that of  $C_f/SiC$  composite (about 36 wt%), as shown in Fig. 7.

#### 4. Conclusions

1. When boron is applied as the active filler, volume shrinkage occurring in the heat-treatment process can be compensated by the volume expansion accompanied in the conversion of boron into h-BN. Therefore, the processing time is shortened by reducing two PIP cycles.
2. The h-BN phase formed in the nitridation process through the in situ reaction between boron and nitrogen disperses homogeneously in the matrix.
3. Some layered crystal structures can be found on the fracture surfaces due to the crack deflection in the h-BN crystal.
4. The oxidation resistance is greatly improved by incorporating boron-bearing species. The weight loss decreases from about 36–16 wt% with the incorporation of boron after being oxidized at  $800^\circ C$  for 10 h.

#### Acknowledgement

This work was supported by the National High Technology Research and Development Program of China (863 Program) under project no. 2006AA03Z565 and Knowledge Innovation Program of the Chinese Academy of Sciences.

#### References

1. Naslain, R., Design, preparation and properties of non-oxide CMCs for application in engines and nuclear reactors: an overview. *Compos. Sci. Technol.*, 2004, **64**, 155–170.
2. Dong, S., Katoh, Y., Kohyama, A., Schwab, S. and Snead, L., Microstructural evolution and mechanical performances of SiC/SiC composites by polymer impregnation/microwave pyrolysis (PIMP) process. *Ceram. Int.*, 2002, **28**, 899–905.
3. Lee, Y. and Radovic, L., Oxidation inhibition effects of phosphorus and boron in different carbon fabrics. *Carbon*, 2003, **41**, 1987–1997.
4. Lamouroux, F., Bertrand, S., Pailler, R., Naslain, R. and Cataldi, M., Oxidation-resistant carbon-fiber-reinforced ceramic-matrix composites. *Compos. Sci. Technol.*, 1999, **59**, 1073–1085.
5. Goujard, S., Vandenbulcke, L. and Tawil, H., Oxidation behavior of 2D and 3D carbon-carbon thermostructural materials protected by CVD polylayer coatings. *Thin Solid Films*, 1994, **252**, 120–130.
6. Goujard, S., Vandenbulcke, L. and Tawil, H., The oxidation behavior of 2-dimensional and 3-dimensional C/SiC thermostructural materials protected by chemical-vapor-deposition polylayers coatings. *J. Mater. Sci.*, 1994, **29**, 6212–6220.
7. Viricelle, J. P., Goursat, P. and Bahloul-Hourlier, D., Oxidation behaviour of a multi-layered ceramic-matrix composite (SiC)(f)/C/(SiBC)(m). *Compos. Sci. Technol.*, 2001, **61**, 607–614.
8. Quemard, L., Rebillat, F., Guette, A., Tawil, H. and Louchet-Pouillier, C., Self-healing mechanisms of a SiC fiber reinforced multi-layered ceramic matrix composite in high pressure steam environments. *J. Eur. Ceram. Soc.*, 2007, **27**, 2085–2094.
9. Naslain, R., Guette, A., Rebillat, F., Pailler, R., Langlais, F. and Bourrat, X., Boron-bearing species in ceramic matrix composites for long-term aerospace applications. *J. Solid State Chem.*, 2004, **177**, 449–456.
10. Tong, C. Q., Cheng, L. F., Yin, X. W., Zhang, L. T. and Xu, Y. D., Oxidation behavior of 2D C/SiC composite modified by  $SiB_4$  particles in inter-bundle pores. *Compos. Sci. Technol.*, 2008, **68**, 602–607.
11. Greil, P., Active-filler-controlled pyrolysis of preceramic polymers. *J. Am. Ceram. Soc.*, 1995, **78**, 835–848.
12. Zhang, G. J., Yang, J. F., Ando, M., Ohji, T. and Kanzaki, S., Mullite-boron nitride composite with high strength and low elasticity. *J. Am. Ceram. Soc.*, 2004, **87**, 296–298.
13. Zhang, G. J., Beppu, Y., Ando, M., Yang, J. F. and Ohji, T., In situ reaction synthesis of silicon carbide-boron nitride composite from silicon nitride-boron oxide-carbon. *J. Am. Ceram. Soc.*, 2002, **85**, 2858–2860.
14. Zhang, G. J. and Ohji, T., In situ reaction synthesis of silicon carbide-boron nitride composites. *J. Am. Ceram. Soc.*, 2001, **84**, 1475–1479.
15. Suttor, D., Erny, T. and Greil, P., Fiber-reinforced ceramic-matrix composites with a polysiloxane/boron-derived matrix. *J. Am. Ceram. Soc.*, 1997, **80**, 1831–1840.
16. Wang, R. G., Pan, W., Chen, J., Jiang, M. N. and Fang, M. H., Fabrication and characterization of machinable  $Si_3N_4/h$ -BN functionally graded materials. *Mater. Res. Bull.*, 2002, **37**, 1269–1277.
17. Cho, W. S., Cho, M. W., Lee, J. H. and Munir, Z. A., Effects of h-BN additive on the microstructure and mechanical properties of AlN-based machinable ceramics. *Mater. Sci. Eng. A*, 2006, **418**, 61–67.